Journal of Ceramic Processing Research. Vol. 12, No. 1, pp. 96~101 (2011)

J O U R N A L O F
Ceramic Processing Research

Study of the factors influencing the immobilization of platinum nanoparticles on multi-walled carbon nanotubes by a polyol process

Jae Woong Jung[a], Chang Young Kim[a], Go Eun Jung[a], Kwang Bo Shim[b], Sung Hoon Jeong[c] and Sung-Chul Yi[a,d]*

[a]*Department of Chemical Engineering, Hanyang University, Haengdang-dong, Seongdong-gu, Seoul 133-791, Republic of Korea*
[b]*Division of Advanced Material Science and Engineering, Hanyang University, Haengdang-dong, Seongdong-gu, Seoul 133-791, Republic of Korea*
[c]*Department of Fiber & Polymer Engineering, Hanyang University, Haengdang-dong, Seongdong-gu, Seoul 133-791, Republic of Korea*
[d]*Fuel Energy Research institute, Hanyang University, Haengdang-dong, Seongdong-gu, Seoul 133-791, Republic of Korea*

The immobilization of platinum (Pt) nanoparticles on the surface of multi-walled carbon nanotubes (MWCNTs) was carried out by a polyol process, with hydroxyl (–OH), carboxyl (–COOH) and carbonyl (C = O) groups on the MWCNTs surfaces formed by an acidic oxidation treatment serving to bind the Pt nanoparticles. The resulting composite nanostructures were characterized through transmission electron microscopy and X-ray diffractometry. Pt nanoparticles that formed on the surfaces of the MWCNTs (Pt/MWCNTs) had an average diameter of ~4 nm. The aggregation and size of these Pt nanoparticles were influenced by the concentration of polyvinylpyrrolidone (PVP, used as a stabilizer), the molecular weight of the PVP and the molar ratio of the reducing agent to Pt ions in the reaction medium. In addition, the concentration of the Pt source (H_2PtCl_6) had a profound influence on the immobilization of the Pt nanoparticles on the surfaces of the MWCNTs. When PVP was present in the solution, the coverage and number of Pt nanoparticles increased with increasing Pt source concentration. However, the degree of aggregation of Pt nanoparticles on the surface of MWCNTs was also increased.

Key words: Pt, Pt/MWCNTs, MWCNTs, Nanoparticles, Polyol process, PVP.

Introduction

Carbon nanotubes have attracted much attention as a support for Pt based catalysts owing to their unique properties, such as high external surface area, electrical and thermal conductivity and good mechanical strength. Furthermore, MWCNT supported Pt catalysts display good catalytic behavior in their fuel cell applications [1-6]. Also, it is well known that the catalytic activity of the Pt nanoparticles is strongly influenced by their size and size distribution. For example, it has been reported that 3-5 nm Pt nanoparticles show a higher electrocatalytic activity for oxygen reduction [7, 8]. Therefore, uniform Pt nanoparticles with precisely controlled sizes are required for high performance catalysts for fuel cell applications. However, producing immobilized Pt nanoparticles with a narrow size distribution and good dispersion over the carbon supports remains a challenge.

The size and size distribution of Pt nanoparticles immobilized on the surface of MWCNTs is influenced by the surface properties of MWCNTs. Since pristine MWCNTs are chemically inert, an acidic oxidation treatment has been employed to functionalize the MWCNTs. An acidic oxidation treatment, such as sonication and refluxing MWCNTs in a concentrated mixture of HNO_3 and H_2SO_4, generates hydroxyl (–OH), carboxyl (–COOH) and carbonyl (C = O) groups on the MWCNT surfaces, serving to bind Pt nanoparticles. In general, the functionalization of MWCNT surfaces could increase the surface binding sites to immobilize metal particles, inhibit the formation of metal agglomerates and improve the metal particle dispersion. However, when Pt/MWCNTs catalysts are prepared by techniques based on the impregnation method and the ion-exchange method [9-13], the particle size distribution of Pt nanoparticles on the surface of CNTs is wide. MWCNT supported Pt catalysts have also been prepared by colloidal and precipitation methods [14-17]. The size and morphology of Pt particles are difficult to control with these methods. On the other hand, more advanced techniques are available, such as sonochemical [18, 19], microwave irradiation [20, 21] and surfactant stabilized methods [22, 23], which have attracted great interest to prepare high-quality MWCNTs supported Pt catalysts.

The addition of a stabilizing agent, such as a polymer or surfactant, can prevent the agglomeration of clusters and the destabilization of the Pt nanoparticles owing to repulsive interaction between the stabilizing agents adsorbed on the surfaces of Pt nanoparticles. PVP which is an amphiphilic, nonionic polymer is commonly employed as a stabilizing agent to prevent agglomeration of colloidal particles in aqueous or non-aqueous solvents; moreover,

*Corresponding author:
Tel : +82-2-2220-0481
Fax: +82-2-2298-5147
E-mail: scyi@hanyang.ac.kr

it also can act as a reducing agent [24]. That is to say, the hydrocarbon chains of PVP cause steric effects between Pt-PVP compounds. Therefore, Pt nanoparticles on the surface of MWCNTs have a narrow size distribution. For example, Hsin *et al*. used PVP as surface functional groups to prepare Pt supported on carbon supports [25]. Chen and co-workers have reported highly dispersed Pt nanoparticles immobilized on carbon black with PVP as a stabilizing agent [26].

In this paper, we report a simple and rapid method for the preparation of Pt nanoparticles immobilized on the surface of MWCNTs using PVP as a stabilizer in the polyol process. Specifically, three parameters were investigated: *(i)* the effects of the molecular weight and concentration of PVP, *(ii)* the effect of Pt salt concentration on the coverage of Pt nanoparticles onto the MWCNTs surfaces, and *(iii)* the effect of the reducing agent concentration on the formation of Pt nanoparticles. Transmission electron microscopy (TEM), energy dispersion X-ray (EDX) and X-ray diffraction (XRD) patterns were employed to characterize the resulting particles.

Experimental

Materials

The MWCNT material which was used as carbon supports had diameters in the rage of 20 to 60 nm and lengths of several micrometre and was obtained from the laboratory of Professor Shim of the Division of Advanced Material Science and Engineering (Hanyang University). The material was synthesized by catalytic vapor deposition (CVD) using a C_2H_2 carbon source with a Fe-Mo/MgO catalyst with over 90 wt % purity [27].

Ethylene glycol (EG, Junsei Chemical Co., Korea) and de-ionized water (Eco-PO&UP, Mirae Scientific Technology Co) were used as solvents. Nitric acid (HNO_3, 60%, Matsunoen chemicals, LTD) and sulfuric acid (H_2SO_4, 97%, Matsunoen chemicals, LTD) were used for the acid treatment process to functionalize MWCNTs surfaces. Hexachloroplatinate (IV) hydrate ($H_2PtCl_6{\cdot}nH_2O$, n = 5.7, Kojima Chemicals Co., Japan) was used as a Pt source, while sodium hydroxide (NaOH, Kanto Chemical Co., Inc.) was used as a reducing agent for Pt ions. Polyvinylpyrrolidone polymers (PVP, Junsei Chemical Co., Japan) with molecular weights of 10,000, 29,000, 40,000 and 58,000 were used as stabilizers and nucleation-promoting agents for the preparation of Pt nanoparticles immobilized on the MWCNT surfaces.

Pretreatment process of MWCNTs

In a typical acidic treatment process, MWCNTs were treated as follows. The pristine MWCNTs in these experiments were added to an acidic solution (concentrated HNO_3-H_2SO_4 in 1 : 2 v/v ratio). The purification and dispersion of MWCNTs in the acid solution were conducted in an ultrasonic bath at 75 ºC for 1 h. Then, the functionalization of MWCNT surfaces was accomplished under refluxing at 93 ºC for 2 h, following a procedure reported in ref 28. After the acid treatment process, functionalized MWCNTs were separated from the acid solution with a centrifuge at 3800 rpm for 30 minutes and washed with deionized water 3 times. Then, functionalized MWCNTs were used to immobilize Pt nanoparticles on their surfaces.

The immobilization of Pt nanoparticles on the MWCNT surfaces

Our strategy for preparation of Pt based catalysts on the MWCNT surfaces is similar to immobilization of Pt nanoparticles on the carbon black in the literature [29]. The immobilization was carried out by reducing the Pt salt precursor, H_2PtCl_6, in the ethylene glycol-water solution (9 : 1 volume ration). Compositions in each set of experimental conditions are summarized in Table 1. In typical experiments, functionalized MWCNTs and the ethylene glycol (EG) solution were added into a 250 ml three neck round bottom flask. The flask was then placed in

Table 1. Experimental conditions for the preparation of Pt/MWCNTs nanocomposite structures

Sample	Molecular weight of PVP	H_2PtCl_6 concentration	PVP concentration	Reducing agent-to-Pt molar ratio [R] species	Pt particle size	Pt loading efficiency
#01	10,000	7.0×10^{-4} m	None	0.5 : 1.0	Agglomeration	-
#02	10,000	7.0×10^{-4} m	0.01 wt%	0.5 : 1.0	Agglomeration	-
#03	10,000	7.0×10^{-4} m	0.03 wt%	0.5 : 1.0	4.28 ± (1.3) nm	24.26 wt%
#04	10,000	7.0×10^{-4} m	0.10 wt%	0.5 : 1.0	3.92 ± (1.0) nm	34.54 wt%
#05	29,000	7.0×10^{-4} m	0.01wt%	0.5 : 1.0	Agglomeration	-
#06	40,000	7.0×10^{-4} m	0.01 wt%	0.5 : 1.0	6.88 ± (1.3) nm	-
#07	58,000	7.0×10^{-4} m	0.01 wt%	0.5 : 1.0	6.23 ± (0.9) nm	-
#08	10,000	7.0×10^{-4} m	0.01wt%	None	Agglomeration	-
#09	10,000	7.0×10^{-4} m	0.01 wt%	2.0 : 1.0	5.29 ± (1.8) nm	-
#10	10,000	7.0×10^{-4} m	0.01 wt%	4.0 : 1.0	4.99 ± (1.9) nm	-
#11	10,000	7.0×10^{-4} m	0.01wt%	0.5 : 1.0	3.43 ± (0.8) nm	-
#12	10,000	3.5×10^{-4} m	0.01 wt%	0.5 : 1.0	4.47 ± (1.5) nm	15.94 wt%
#13	10,000	5.3×10^{-4} m	0.01 wt%	0.5 : 1.0	4.59 ± (1.3) nm	20.93 wt%

*Pt loading efficiency was analyzed using SEM-EDX

an ultrasonic bath for 10 minutes to disperse the MWCNTs in the EG solution, followed by the dissolution of PVP in the mixture through mild stirring to prevent the distortion of the polymer chain. After dissolving PVP, H_2PtCl_6 and a reducing agent were added to the solution, which was then refluxed at 138 °C for 3 h with magnetic stirring.

Characterization

The metal contents were determined by EDX on a JEOL JSM-5600LV scanning electron microscope (SEM). Morphological properties of the Pt nanoparticles immobilized on the surface of MWCNTs were characterized by TEM using on Jeol JEM-2000EX II operating at 200 kV. Each specimen for TEM analysis was prepared by placing a drop of a diluted solution of a colloidal sample in ethanol onto a TEM grid (a copper grid pre-coated with amorphous carbon), which was then dried in an oven at 40 °C for 24 h prior to observation.

XRD was used to examine the crystallinity/crystal structure and phase constituents of samples prepared by the polyol processes. The XRD measurements were performed with powders packed completely in the holder of a Rigaku D/MAX RINT 2500 X-ray diffractometer operated at 40 kV and 100 mA. The incident wavelength was Cu K λ = 1.5406 Å and the detector moved step by step ($\Delta 2\theta = 0.05^o$) between 10° and 90°. The scan speed was 4° minute^{1}.

Results and Discussion

It is well known that pristine MWCNTs contain impurities such as Fe-Mo/MgO, which are used as catalysts to synthesize the carbon nanotubes. Also, the surface of pristine MWCNTs is chemically inert. Therefore, it is necessary to conduct an acidic oxidation treatment to purify and functionalize the pristine MWCNTs before use. As a result of the acidic oxidation treatment under a reflux condition with a H_2SO_4-HNO_3 mixture, the surface of MWCNTs are functionalized with hydroxyl, carboxyl and carbonyl groups which are used as nucleation sites during the Pt formation period that is similar to the role of seed materials in heterogeneous nucleation techniques.

In our experiment, Pt nanoparticles are immobilized on the surface of MWCNTs by a polyol process in the presence of PVP. Ethylene glycol is commonly used in polyol processes because of its high dielectric constant and high reducing power. At high temperatures, ethylene glycol decomposes to generate reducing species for the formation of platinum nanoparticles by the reduction of the platinum ions. The equation for the reduction mechanism by ethylene glycol is described as follows [30] :

$$2CH_2OHCH_2OH \rightarrow 2CH_3CHO + 2H_2O \quad (1)$$

$$2CH_3CHO + (PtCl_6)^{2-} + 6OH^- \rightarrow 2CH_3COO^- + Pt^0 + 6Cl^- + 4H_2O \quad (2)$$

Figs. 1 and 2 display the results of the characterization

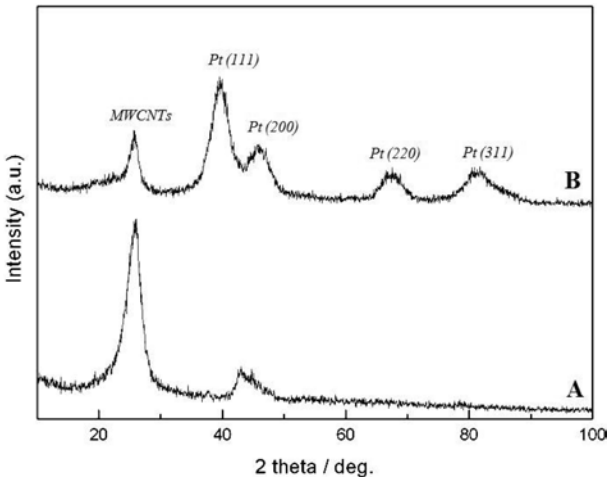

Fig. 1. The X-ray diffraction (XRD) pattern of (A) Pristine MWCNTs and (B) Pt/MWCNTs (#03).

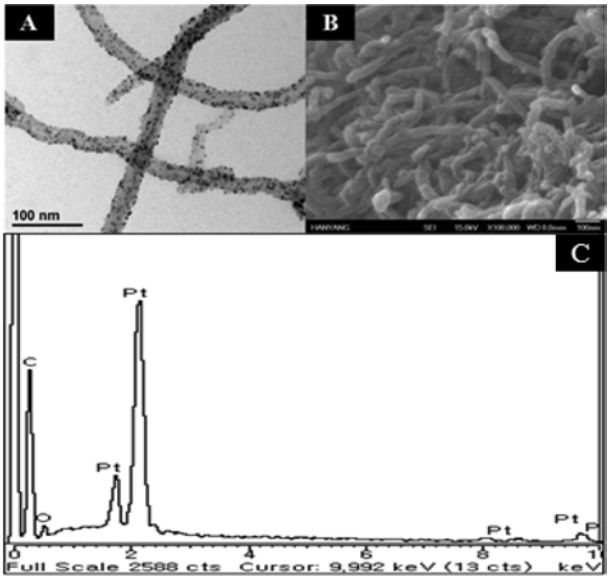

Fig. 2. A: TEM image of Pt/MWCNTs, B: SEM image of Pt/MWCNTs and C: EDX spectra of Pt/MWCNTs (#03).

of the Pt/MWCNTs nanocomposite structure (sample: #03) by XRD, TEM and EDX spectra by SEM. The powder XRD pattern for Pt/MWCNTs is shown in Fig. 1 alongside the diffraction pattern of pristine MWCNTs for comparison. It clearly shows the four characteristic peaks of Pt with face-center the cubic (f.c.c.) structure. The strongest diffraction peak is located at a 2θ value of 39.57° (111), and the other strong diffraction peaks are located at 45.95°(200), 67.55°(220) and 81.60°(311), respectively. These indicate the successful reduction of Pt ions to Pt nanoparticles. Also, the broader diffraction peaks for the Pt/MWCNTs illustrate the smaller average particle sizes as calculated by the Scherrer equation [31] :

$$L = \frac{0.9\lambda_{k\alpha 1}}{B_{(2\theta)} cos\theta_B} \quad (3)$$

where L is the average particle size, $\lambda_{k\alpha 1}$ is the X-ray

wavelength (1.54056 Å for Cu $k\alpha 1$ radiation), $B_{2\theta}$ is the half-peak width and θ_B *is* the angle corresponding to the peak maximum.

Calculation results using the half-peak width for the Pt (220) plane give the average size of the Pt nanoparticles as 3.8 ± 0.3 nm. The diffraction peak at 2θ of 25.75° is attributed to the presence of MWCNTs with a graphite structure. Fig. 2. A. shows a typical TEM image of the Pt nanoparticles immobilized on MWCNTs prepared by the polyol process. The Pt nanoparticles are dispersed uniformly on the sidewalls of the MWCNTs and an agglomeration of Pt nanoparticles is rarely observed. The average particle size is ~4 nm, which is in good agreement with the XRD result (3.8 ± 0.3 nm) that was calculated according to the XRD data. The EDX spectra in the SEM (Fig. 2(C)) shows a Pt content of 24.26 wt% for Pt/MWCNTs. Based on the TEM images and XRD results, the Pt nanoparticles immobilized on the MWCNTs are small and have a small size distribution, which could be attributed to the preparation method which employs a stabilizing agent.

To investigate the effect of the concentration of PVP on the formation of Pt nanoparticles, the short-chain PVP (Mw = 10,000) was added to the system and at concentrations of 0, 0.01 wt%, 0.03 wt% and 0.10 wt% as summarized in Table 1, sample #01~04. Fig. 3 displays the TEM image of the Pt nanoparticles supported on MWCNTs prepared at these four concentrations by the polyol process. When PVP was not present in the solution, agglomeration consisting of small Pt nanoparticles occurred and Pt nanoparticles were rarely immobilized on the functionalized MWCNT surfaces (Fig. 3(A)). Thus, protecting groups in the stabilizing agents were needed to prevent agglomeration. PVP has a polyvinyl backbone with polar groups. The donated lone pairs of both nitrogen and oxygen atoms in the polar groups of a PVP unit may attach homogeneously to Pt nanoparticles and Pt ions. Therefore, the surface of Pt nanoparticles covered with PVP via physical and chemical bonding inhibits inter-particle contact and thus, agglomeration of the metal particles [32]. In our experiment, when PVP is added in the solution, the degree of agglomeration of Pt nanoparticles was decreased and the average diameter of Pt nanoparticles immobilized on the MWCNTs surface also decreased with an increase in the concentration of PVP. However, the generation of free Pt nanoparticles, i.e., those not immobilized on the functionalized MWCNTs surfaces was observed when the concentration of PVP was 0.10 ^{wt}% or more (Fig. 3(B)-(D)).

Fig. 4 reveals the influence of different molecular weights of PVP (Mw = 10,000, 29,000, 40,000 and 58,000) on the formation of Pt nanoparticles immobilized on functionalized MWCNTs. The TEM images indicate that the degree of agglomeration and coverage of Pt nanoparticles decreased with an increase in the molecular weight of PVP. When short-chain PVP (Mw = 10,000) was used, there were more opportunities for seed growth because of the short polymer chain. Therefore, the agglomeration of Pt nanoparticles occurred on the MWCNT surfaces. On the other hand, as the molecular weight of the PVP increased, the physical barrier to seed growth was increased due to the steric effects of the long chain polymer and, thus, the degree of agglomeration and coverage of Pt nanoparticles decreased.

PVP plays an important role in the formation of metal particles; it behaves as a protecting agent and reducing agent. In previous studies, PVP had been used to synthesize Ag nanoparticles and Ag/SiO_2 nanocomposite particles using a modified alcohol reducing process [33, 34]; the PVP concentration influenced the reduction rates of the metal ions, which affected the resulting nanoparticles. On the other hand, the Pt ions were also reduced on the MWCNT surfaces using several reducing agents such as NaOH. The content of NaOH in the ethylene glycol solution (i.e., the pH) influenced the average size and size distribution of Pt nanoparticles prepared by the polyol process [35, 36].

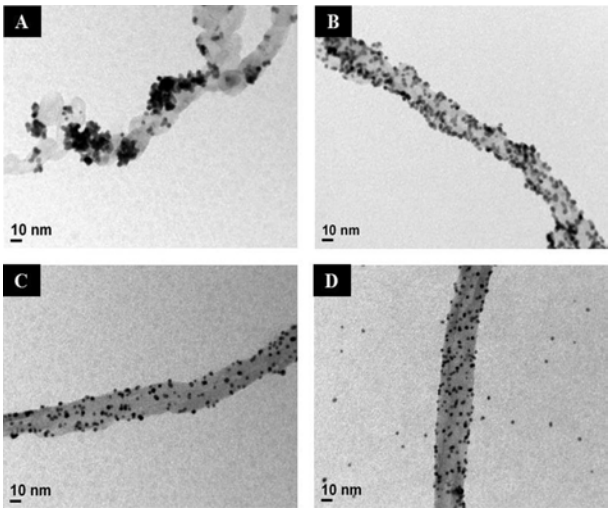

Fig. 3. TEM images of the Pt/MWCNTs nanocomposite structures prepared by the polyol process in the presence of PVP (M.W. = 10,000) at various concentrations (A: #01, B: #02, C: #03 and D: #04).

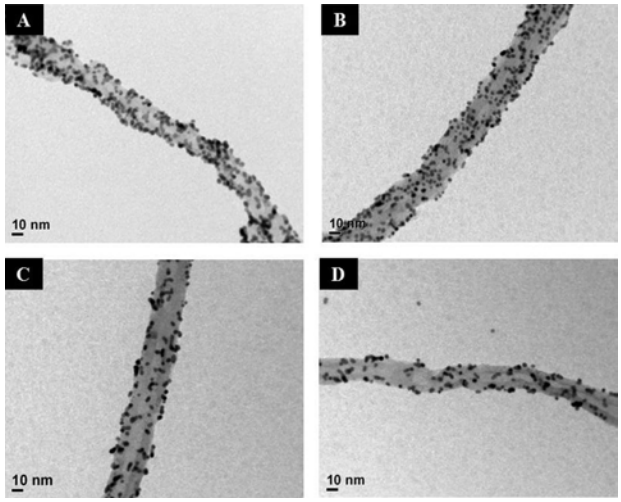

Fig. 4. TEM images of the Pt/MWCNTs nanocomposite structures prepared by the polyol process in the presence of various molecular weights of PVP (A:# 02, B:# 05, C:# 06 and D: #07).

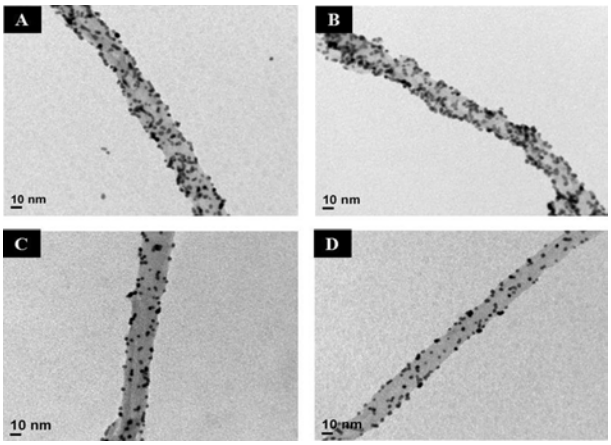

Fig. 5. TEM images of the Pt/MWCNTs nanocomposite structures prepared by the polyol process in the presence of reducing agent (NaOH) at various concentrations (A: #08, B: #02, C: #09 and D: #10).

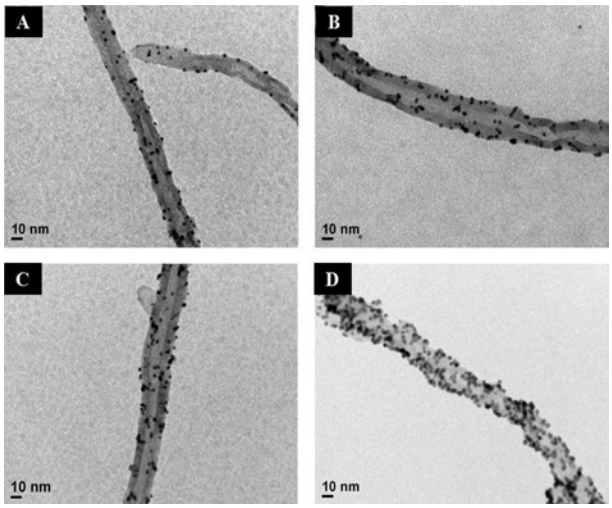

Fig. 6. TEM images of the Pt/MWCNTs nanocomposite structures prepared by the polyol process in the presence of Pt source (H_2PtCl_6) at various concentrations (A: #11, B: #12, C: #13 and D: #02).

Fig. 5 displays the effect of the reducing agent on the formation of Pt nanoparticles on MWCNT surfaces when the reducing agent-to-Pt molar ratio [R] was varied from 0 to 4.0. In general, an increase in the concentration of the reducing agent increases the rate of reduction of metal ions, leading to the formation of smaller metal particles at low colloidal metal concentrations [37]. As seen in Fig. 5, when the concentration of NaOH is not sufficient to increase the reduction rate of Pt ions, agglomeration of Pt nanoparticles is observed due to the long period of nuclei growth (Fig. 5(A), (B)). However, as the concentration of NaOH is increased, the degree of agglomeration and the coverage of Pt nanoparticles immobilized on the MWCNT surfaces decreased. This phenomenon indicates that (i) the reduction of Pt ions by the reducing agent produces more Pt nuclei within a shorter period, (ii) the growth rate of Pt nanoparticles is decreased, and (iii) that nucleation and growth are separate processes. In other words, small Pt particles with narrow size distributions are generated owing to the rapid reduction of Pt ions. Therefore, the agglomeration of Pt nanoparticles is prevented with an increased concentration of reducing agent.

To investigate the effect of Pt ion concentration on the formation of Pt nanoparticles immobilized on the surface of functionalized MWCNTs, different amounts of Pt solution were added to the system. Fig. 6 shows the TEM images of Pt nanoparticles supported on functionalized MWCNTs with different concentrations of Pt salts by the polyol process. The average diameter and coverage of Pt nanoparticles immobilized on the MWCNT surfaces are influenced by the number densities of functional sites on the surface. That is to say, when the available surface sites for Pt immobilization are saturated, particles can only grow bigger [28]. Therefore, the size and coverage of Pt nanoparticles can also be controlled by the concentration of the Pt salt in the system. Based on these images, when the concentration of the Pt salt, H_2PtCL_6, was increased, the size and the coverage of Pt nanoparticles immobilized on the MWCNTs surfaces also increased. However, when a relatively high concentration of the Pt salt (7.0×10^{-4} m or more) is added into the system, agglomeration of Pt nanoparticles immobilized on the MWCNTs surfaces occurred (Fig. 6(D)). By contrast, Pt nanoparticles are well dispersed on the MWCNT surfaces and the degree of agglomeration is decreased when the concentration of the Pt salt is relatively low.

Conclusions

In summary, Pt/MWCNTs nanocomposite structures can be prepared by a polyol process in the presence of functionalized MWCNTs resulting in Pt nanoparticles attached to the MWCNTs surfaces. The surfaces of MWCNTs were functionalized with hydroxyl (–OH), carboxyl (–COOH) and carbonyl (C = O) groups by an acidic oxidation treatment and acted as a nucleation site during the formation of Pt particles.

Formation of Pt nanoparticles on the MWCNTs surface is influenced by the molecular weight of the PVP and the concentration of PVP, reducing agent and Pt precursor. The absence of PVP was unfavorable for the formation of Pt particles on the MWCNTs surfaces. When PVP had a low molecular weight of 10,000 and was added at a relatively high concentration of 0.03 wt%, Pt nanoparticles were deposited favorably on the MWCNTs surfaces. In addition, the concentration of the reducing agent affected the reduction rate of the Pt ions, thereby determining the degree of agglomeration and coverage of Pt nanoparticles immobilized on the MWCNT surfaces.

Acknowledgment

This study is supported by the Manpower Development Program for Energy & Resources supported by the Ministry of Knowledge and Economy (MKE), Republic of Korea.

References

1. C.C. Chen, C.F. Chen, C.M. Chen and F.T. Chuang, Electrochem. Commun. 9 (2007) 159-163.
2. Y. Mu, H. Liang, J. Hu, L. Jiang and L. Wan, J. Phys. Chem. B 109 (2005) 22212-2216.
3. D.J. Guo and H.L. Li, Electroanalysis 17 (2005) 869-872.
4. T. Matsumoto, T. Komatsu, H. Nakano, K. Arai, Y. Nagashima, E. Yoo, T. Yamazaki, M. Kijima, H. Shimizu, Y. Takasawa and J. Nakamura, Catal. Today. 90 (2004) 277-281.
5. S. Wang, S.P. Jiang, T.J. White, J. Guo and X. Wang, J. Phys. Chem. C 113 (2009) 18935-18945.
6. Z.Q. Tian, S.P. Jiang, Y.M. Liang and P.K. Shen, J. Phys. Chem. B 110 (2005) 5343-5350.
7. K. Kinoshita, J. Electrochem. Soc. 137 (1990) 845-848.
8. M. Peuckert, T. Yoneda, R.A.D. Betta and M. Boudart, J. Electrochem. Soc. 133 (1986) 944-947.
9. B. Xue, P. Chen, Q. Hong, J. Lin and K.L. Tan, J. Mater .Chem. 11 (2001) 2378-2381.
10. G. L. Che, B.B. Lakshmi, E.R. Fisher and C.R. Martin, Nature 393 (1998) 346-349.
11. B. Rajesh, K.R. Thampi, J.M. Bonard, N. Xanthopoulos, H.J. Mathieu and B. Viswanathan, J. Phys. Chem. B 107 (2003) 2701-2708.
12. T. Matsumoto, T. Komatsu, K. Arai, T. Yamazaki, M. Kijima, H. Shimizu, Y. Takasawa and J. Nakamura, Chem. Commun. 7 (2004) 840-841.
13. R.Q. Yu, L.W. Chen, Q.P. Liu, J.Y. Lin, K.L. Tan, S.C. Ng, H.S.O. Chan, G.Q. Xu and T.S.A. Hor, Chem. Mater. 10 (1998) 718-722.
14. V. Lordi and N. Yao, J. Wei, Chem. Mater. 13 (2001) 733-737.
15. Z.L. Liu, X.H. Lin, J.Y. Lee, W. Zhang, M. Han and L.M. Gan, Langmuir 18 (2002) 4054-4060.
16. B.C. Satishkumar, E.M. Vogl, A. Govindaraj and C.N.R. Rao, J. Phys. D 29 (1996) 3173-3176.
17. X. Li, S. Ge, C.L. Hui and I.M. Hsing, Electrochem. Solid-State Lett. 7 (2004) A286-A289.
18. H. Tong, H.L. Li and X.G. Zhang, Carbon 45 (2007) 2424-2432.
19. Z.C. Wang, D.D. Zhao, G.Y. Zhao and H.L. Li, J. Solid State Electrochem. 13 (2009) 371-376.
20. X. Li, W. X. Chen, J. Zhao, W. Xing and Z.D. Xu, Carbon 43 (2005) 2168-2174.
21. W. Chen, J. Zhao, J.Y. Lee and Z. Liu, Mater. Chem. Phys. 91 (2005) 124-129.
22. H. Bönnemann, G. Braun, W. Brijoux, R. Brinkmann, A.S. Tilling, K. Seevogel, K. Siepen and J. Organomet. Chem. 520 (1996) 143-162.
23. P.L. Kuo, C.C. Chen and M.W. Jao, J. Phys. Chem. B 109 (2005) 9445-9450.
24. P. Toneguzzo, G. Viau, O. Acher, F. Fiévet-Vincent and F. Fiévet, Adv. Mater. 10 (1998) 1032-1035.
25. Y.L. Hsin, K.C. Hwang and C.T. Yeh, J. AM. CHEM. SOC. 129 (2007) 9999-10010.
26. W.X. Chen, J.Y. Lee and Z. Liu, Chem. Commun. (2002) 2588-2589.
27. W.S. Kim, S.Y. Moon, S.Y. Bang, B.G. Choi, H. Ham, T. Sekino, K.B. Shim, Appl. Phys. Lett. 95 (2009) 083103.
28. Y. Xing, J. Phys. Chem. B 108 (2004) 19255-19259.
29. M. Chen and Y. Xing, Lanmuir 21 (2005) 9334-9338.
30. J. Yang, T.C. Deivaraj, H.P. Too and J.Y. Lee, Lanmuir 20 (2004) 4241-4245.
31. V. Radmilovic, H.A. Gasteiger and P.N. Ross Jr., J. Catal. 154 (1995) 98-106.
32. Z. Zhang, B. Zhao and L. Hu, J. Solid State Chem. 121 (1996) 105-110.
33. C.Y. Kim, B.M. Kim, S.H. Jeong and S.C. Yi, J. Ceram. Process. Res. 7 (2006) 241-244.
34. C.Y. Kim, S.H. Jeong and S.C. Yi, J. Ceram. Process. Res. 8 (2007) 445-449.
35. W. Yu, W. Tu and H. Liu, Langmuir 15 (1999) 6-9.
36. C. Bock, C. Paquet, M. Couillard, G.A. Botton and B.R. MacDougall, J. am. chem. soc, 126 (2004) 8028-8037.
37. T. Teranishi, and M. Miyake, Chem. Mater. 10 (1998) 594-600.